Supporting information

Polyglutamic Acid-Coordinated Assembly of Hydroxyapatite Nanoparticle for Synergistic Tumor-specific Therapy

Ma Xiaoyu[a,b], Dong Xiuling[c], Zang Chunyu[c], Sun Yi[c], Qian Jiangchao[c], Yuan Yuan*[a,b,c]and Liu Changsheng*[a,b,c]

a. Key Laboratory for Ultrafine Materials of Ministry of Education, East China University of Science and Technology, Shanghai 200237, P R China

b. Engineering Research Center for Biomedical Materials of Ministry of Education, East China University of Science and Technology, Shanghai 200237, P R China

c. The State Key Laboratory of Bioreactor Engineering, East China University of Science and Technology, Shanghai 200237, P R China

E-mail: yyuan@ecust.edu.cn; liucs@ecust.edu.cn

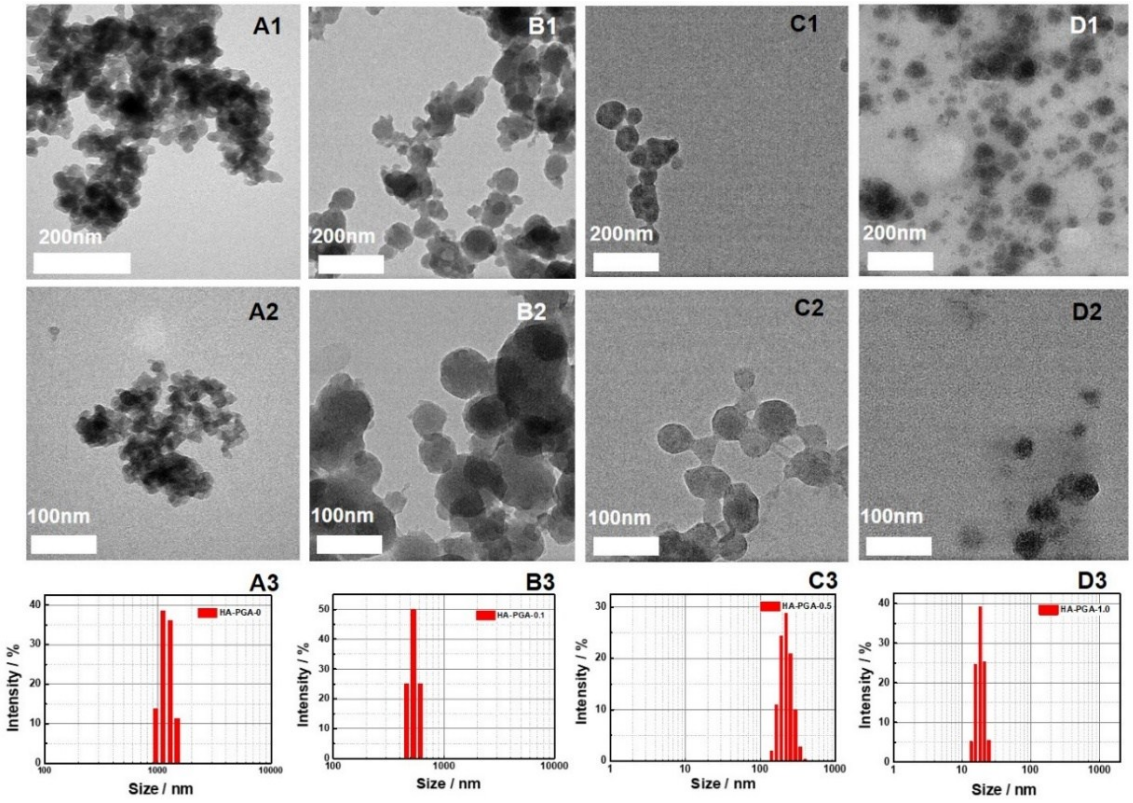

Figure S1. TEM observation of (A1-A2) HA, (B1-B2) HA-PGA-0.1 g, (C1-C2) HA-PGA-0.5 g and (D1-D2) HA-PGA-1.0 g; A3-D3: DLS tests for HA-PGA with different PGA addition (0, 0.1, 0.5, 1.0 g)

From 0 to 1.0 g, the increase in PGA addition could greatly reduce the size of hybrid HAp. The size and size distribution significantly varied at different PGA addition amount as the particles in control group without PGA addition were of quasi-spherical shape and suffered from great agglomeration while the product particles were of spherical shape with good integrity when PGA was introduced into the system. By increasing the PGA amount, the size of resultant particles decreased to around 30 nm in Figure S1D, and the dispersibility gradually increased. Additionally, DLS was also applied to determine the size change of PGA-stabilized particles. Compared with the particle size directly seen in TEM, slight agglomeration was observed in the DLS results for all groups, mainly due to the intrinsic nature of nano-sized calcium phosphate, whose high surface energy will easily lead to the generation of clusters via hydrogen bond and crystalline bridges in the water phase. Nonetheless, the size of HA-PGA hybrids was far less than that of pure HA, exhibiting the role played by PGA in the control over particle size and dispersibility maintainance.

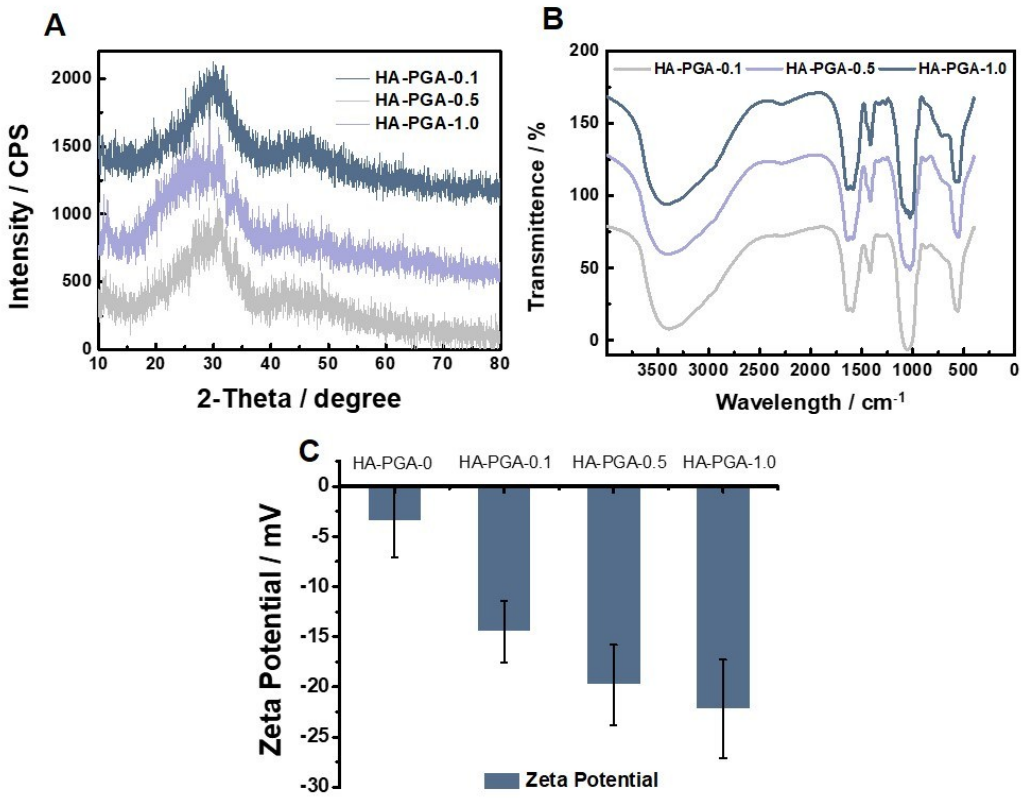

Figure S2. (A) XRD patterns; (B) FT-IR spectrum; and (C) zeta potential of resultant HA-PGA particles with various PGA amount

XRD and FT-IR were utilized to further examine the physicochemical properties. It could be seen that the addition of PGA into calcium phosphate via precipitation process led to a relatively low crystallinity. A supplemental test of ICP-MS was carried out to detect the ratio of Ca and P, which was around 1.62, similar to that of hydroxyapatite. In B, typical CaP phase composition was identified by FTIR spectra. In addition, zeta potentials of the HA-PGA particles were also examined, showing a steady increase with the addition of PGA amount, due to the confinement of more PGA in the hybrid and promoted deprotonation in the solution.

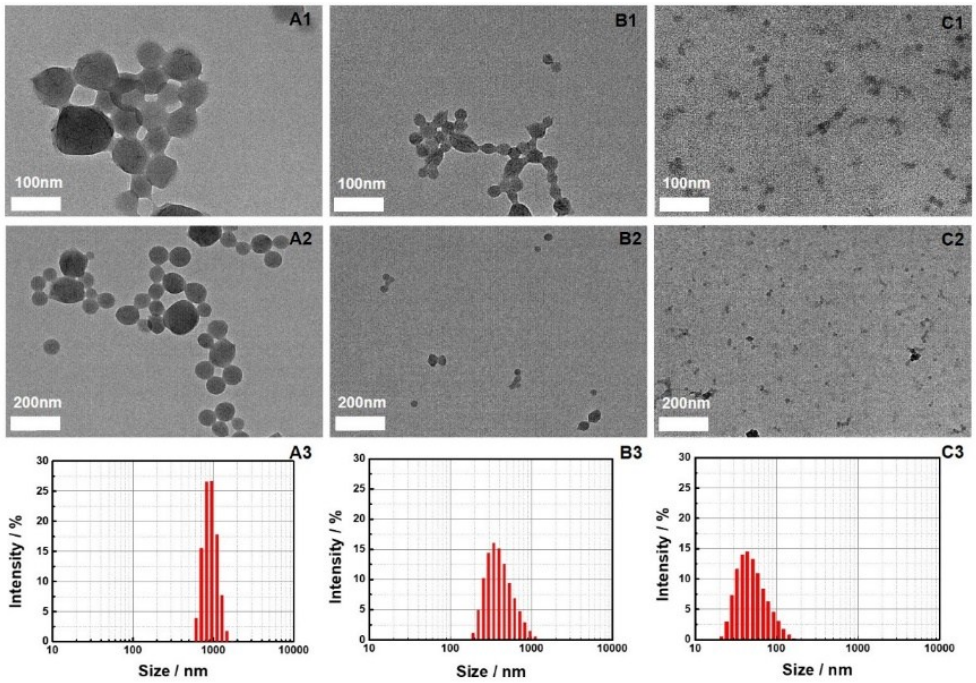

Figure S3. TEM observations of resultant nano-particles at different precursor concentrations (identified with PGA) A1, A2: 2.9 mg/mL(high); B1,B2: 1.6 mg/mL(medium); C1,C2: 0.8 mg/mL(low); A3-C3: DLS tests for corresponding particles

The Ca/P/PGA ratio was fixed at 0.7/0.23/1.0 g according to the above composition of HA-PGA-1.0, but the precursor concentration was adjusted to 0.8, 1.6, 2.9 $mg \cdot ml^{-1}$. All samples exhibited intact spherical shape, but sizes varied greatly at different concentrations. At higher point of 2.9 $mg \cdot ml^{-1}$, particles within 80-100 nm prevailed while a lower initial reaction concentration would result in a shrink in particle size, where the minimum particle size could reach 10-20 nm. A relatively low reaction concentration would significantly reduce the chance of nucleus collision to prevent the growth and merge. Besides, DLS was employed to confirm the change in particle size in Figure S3(A3-C3). Though the hydrated radius was larger than that observed in TEM due to swelling of modified polymer and bridging in water, the trend in size change was well accorded with the TEM observation.

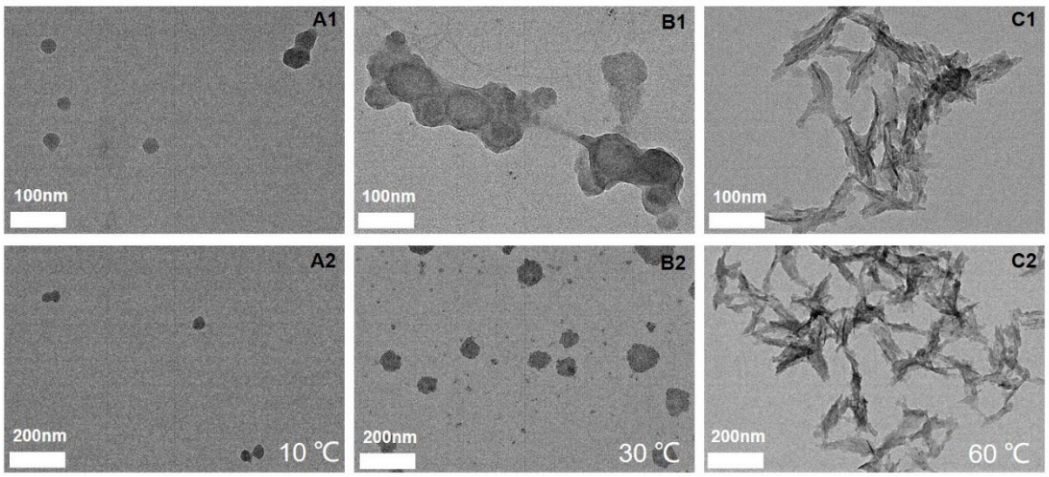

Figure S4. TEM observations of resultant nano-particles at different reaction temperature A:10°C; B: 30°C; C:60°C;

The reaction temperature was tuned to reveal its effect on subsequent particle size and morphology for HA-PGA-1.0. With the increase of reaction temperature from 10 °C-30 °C, the size of particles enlarged from 20 nm to 80-100 nm. It was worth to note that the spherical shape of particles transferred into needle or rod-like when the reaction temperature reached 60°C.

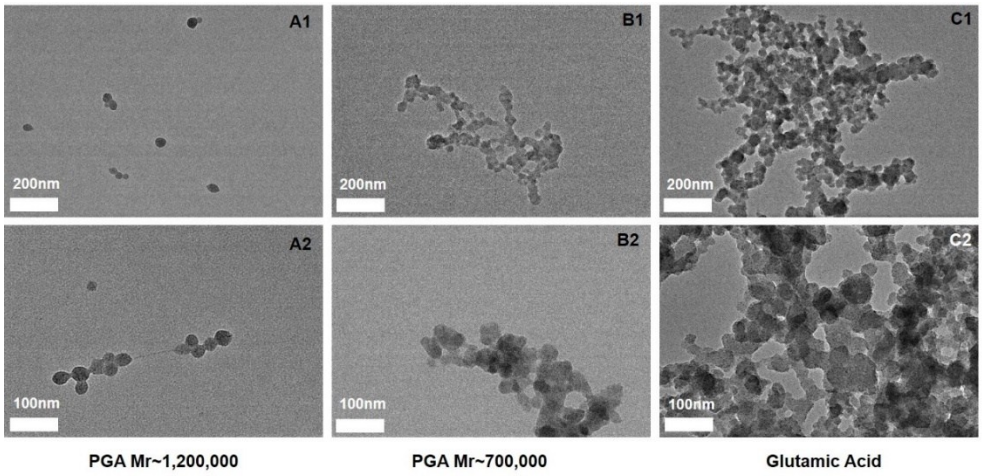

Figure S5. TEM observations of resultant PGA-HA nano-particles with different PGA molecular weight/GA A: 1,200,000; B: 700,000; C: GA monomer

Molecular weight of PGA was also varied to determine the influence of polycarboxylic polymer on the size and morphology of obtained particles, as the temperature, precursor concentration and PGA addition amount were fixed. With the addition of GA/PGA, the obtained particles maintained spherical in shape, within the size range of 20-40 nm. However, it could be clearly seen that the polymer with larger molecular weight led to better dispersibility, regularity and uniformity.

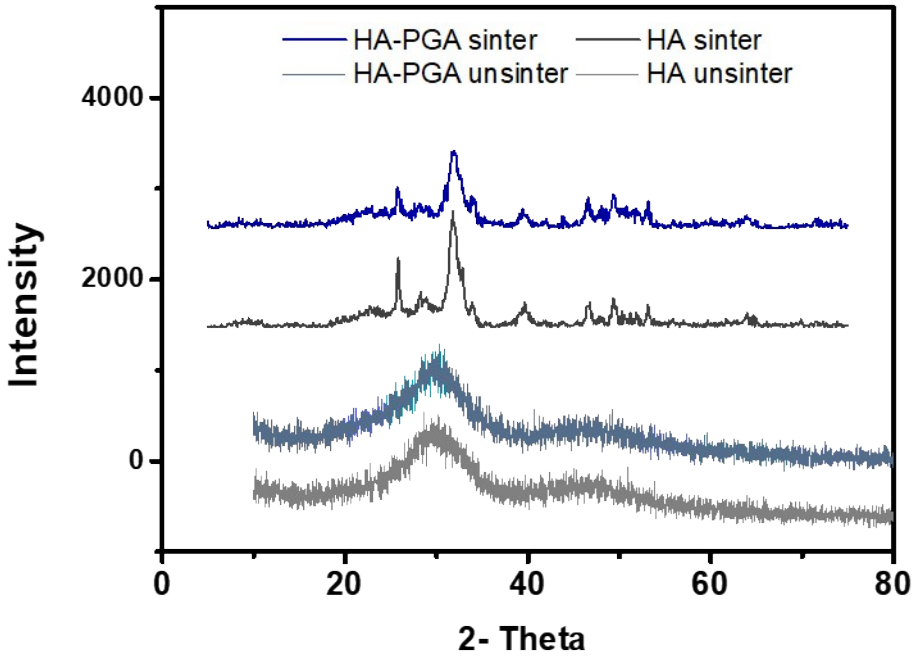

Figure S6. XRD of traditional HA and HA-PGA with and without sintering

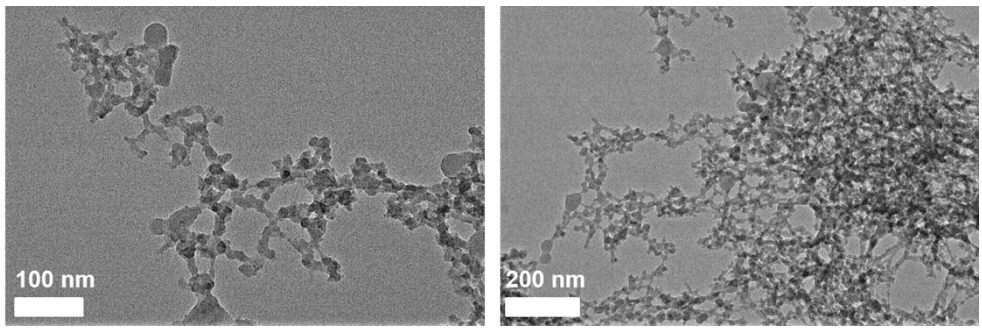

Figure S7. TEM observation of HA nano-particles prepared by PGA addition after CaP formation

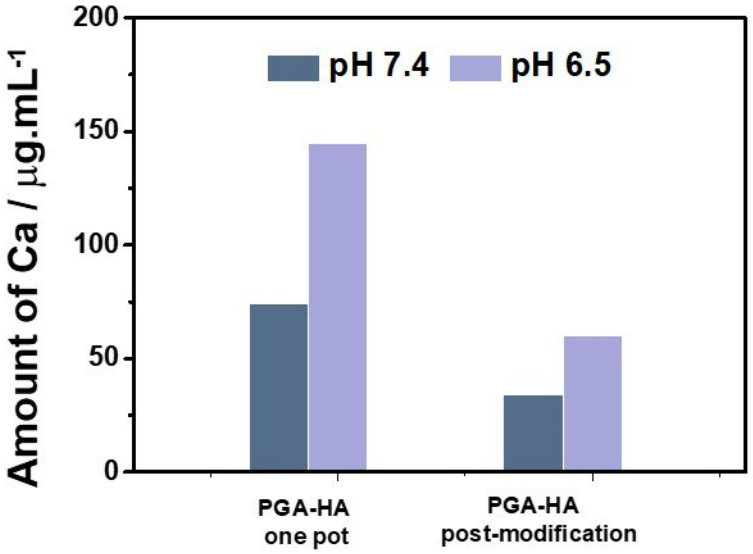

Figure S8. Amount of Ca^{2+} dissolution for 24 hr under various pH conditions measured by ICP

Table S1. The synthesis parameters and the characterization of obtained particles

	Synthesis parameters in the reaction					Characterization	
	Concentration （mg/mL）	PGA Amount (g)	Reaction temperature (°C)	PGA molecular weight	Reaction Time (hr)	Size (nm)	Morphology
1	1.6	0.1	10	1,200,000	24	80-100	Spherical-like
2	1.6	0.5	10	1,200,000	24	40-50	Spherical
3	1.6	1.0	10	1,200,000	24	20-30	Spherical
4	0.8	1.0	10	1,200,000	24	10-20	Spherical
5	2.9	1.0	10	1,200,000	24	80-100	Spherical
6	1.6	1.0	30	1,200,000	24	50-60	Spherical
7	1.6	1.0	60	1,200,000	24	100-150	Rod-like
8	1.6	1.0	10	700, 000	24	20-30	Ellipsoid/Spherical
9	1.6	1.0	10	GA monomer	24	30-80	Spherical-like/ Irregular
10	1.6	1.0	10	1,200,000	0.5	<10	Spherical
11	1.6	1.0	10	1,200,000	8	~30	Spherical

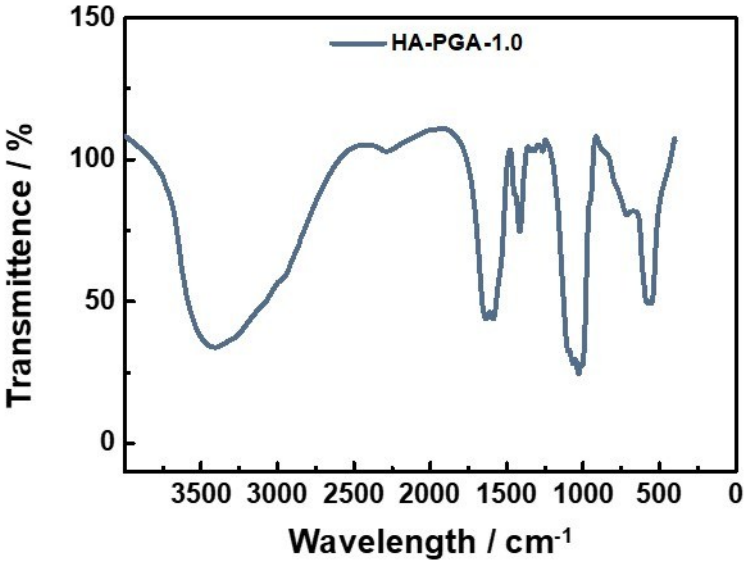

Figure S9 FT-IR spectrum of HA-PGA-1.0

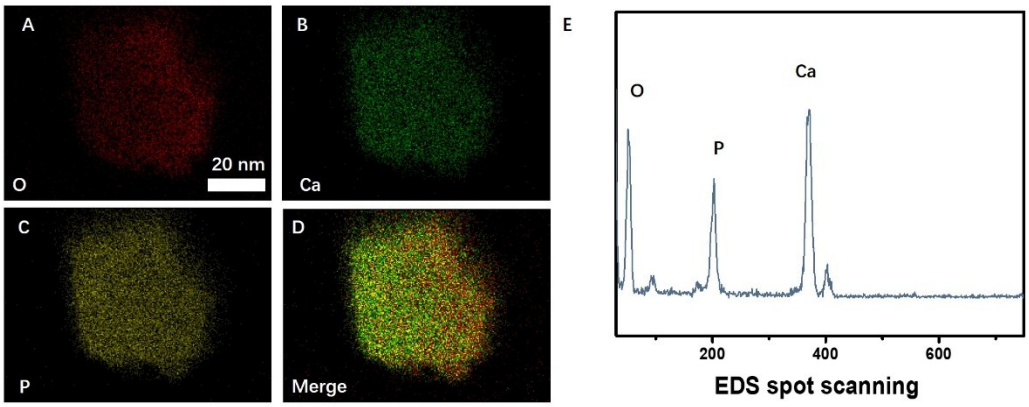

Figure S10 A-D:EDS mapping of HA-PGA NPs；E：Spot scanning of HA-PGA NPs

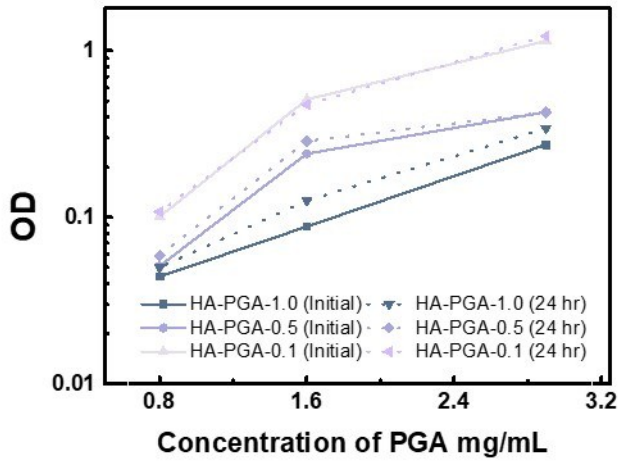

Figure S11 OD values for HA-PGA-0.1/0.5/1.0 under various precursor concentration

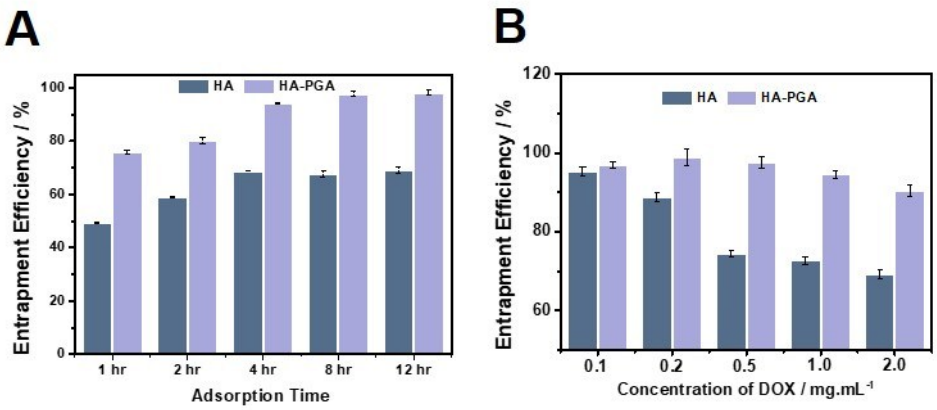

Figure S12 A: Loading profiles of HA and HA-PGA at different adsorption time; B: Loading profiles of HA and HA-PGA at different initial DOX concentration

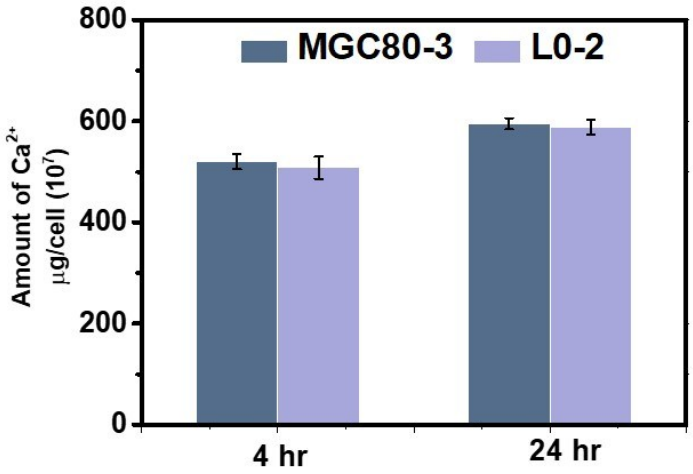

Figure S13 Internalization of PGA-HA in tumor and normal cell lines at 4 and 24 hr

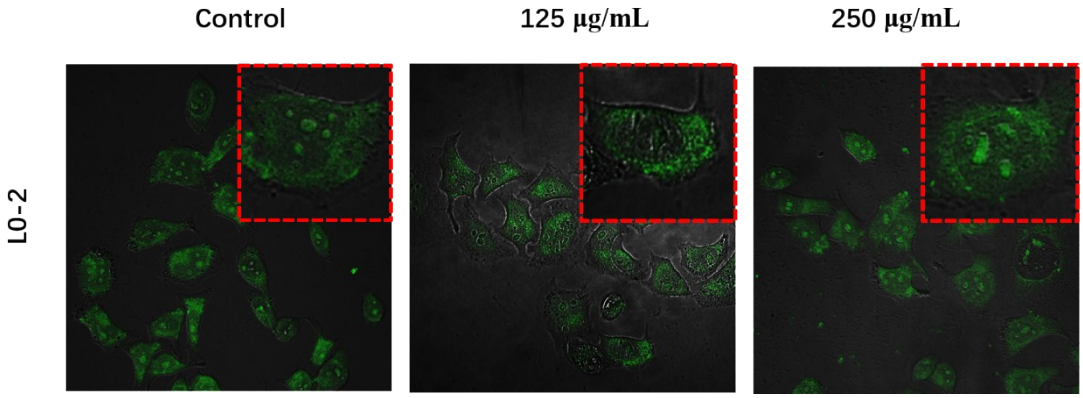

Figure S14 CLSM images of intracellular Ca^{2+} under different HA-PGA addition in L0-2

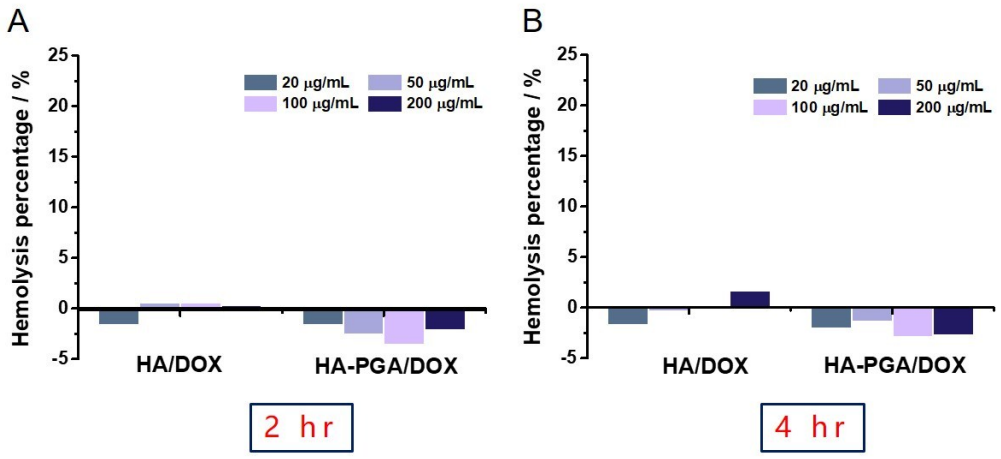

Figure S15. Hemolysis percentage of HA/DOX and HA-PGA/DOX

The study was carried out in strict compliance with the NIH guidelines for the care and use of laboratory animals (NIH Publication No. 85e23 Rev. 1985) and was approved by the Research Center for Laboratory Animal of Shanghai University of Traditional Chinese Medicine.